LOW-COST LIFE ASSESSMENT OF LIQUID ROCKET ENGINES

by replacing full-scale engine tests with TMF panel tests

P. H. KRINGE, J. R. RICCUS & M. OSCHWALD, DLR Institute of Space Propulsion, Im Langen Grund, 74239 Hardthausen, Germany

Email pascal.kringe@dlr.de

Liquid rocket engines are still key components of many space transportation systems. The combustion chamber of the engine itself is one of the most critical parts as it has to withstand severe temperatures, extreme temperature gradients and high pressures. Reusability and therefore cyclic loading can lead to failure due to rupture of the cooling channels in the inner liner of the combustion chamber. Those failures are induced by a progressing failure mechanism called doghouse effect. The doghouse effect causes thinning of the cooling channels until rupture. For the development of new engines numerical methods are used. In order to save costs for obtaining experimental data to validate numerical analysis methods, a Thermo-Mechanical Fatigue (TMF) test bench was set up at the Lampoldshausen site of German Aerospace Center (DLR) to reduce the need for expensive full scale rocket engine tests. The test bench uses so-called thermomechanical fatigue panels representing a small section of the geometry (5 - 7 cooling channels) of the hot gas wall. To simulate the heat load, a diode laser can provide thermal loading with heat fluxes up to $\dot{q}$ = 25 MW/m² applied to an area of 10 mm x 34 mm. Supercritical Nitrogen at a temperature of T = 160 K and a pressure of p = 50 bar serves as coolant. The laser is cyclically powered on for typically 200 s until rupture is visible. The heat distribution on the laser-loaded surface of the TMF panel is measured with an infrared camera. The fatigue life is assessed by counting the number of laser cycles. With this method the appropriateness and response of different copper based alloys can be predicted for different use-cases like liquid core stage engines, liquid booster engines or liquid upper stage engines regarding thermomechanical fatigue by utilizing a cost-saving alternative to full scale rocket engine tests. This paper presents the detailed capabilities and potential of the TMF panel test bench at DLR Lampoldshausen as well as the recent results of a TMF panel made of CuCrZr alloy.

Keywords: Thermo-Mechanical Fatigue, TMF panel test, Liquid Rocket Engine, Doghouse Effect

1 INTRODUCTION

The sources of validation data including CFD, thermal, structural FEM analyses and material parameters for the life estimation of rocket engines are rare and not very well shared. Furthermore, the creation of additional data is very expensive.

Therefore at DLR Lampoldshausen the TMF panel test bench was developed. It is capable of generating close-to-reality data for the validation of numerical models for CFD, thermal and structural analysis as well as material behavior by using so-called thermomechanical fatigue (TMF) panels. These TMF panels represent only a small cutout of the inner liner of a combustion chamber of a liquid rocket engine (LRE), typically the size of 5–7 cooling channels. Cyclic laser heating of the surfaces represents the hot gas and provides the heat flux. This is adequate to simulate the so-called doghouse effect and the effects of typical failure mechanisms in LREs and thus reducing the need of full scale tests with actual combustion.

This paper was first presented at the 17th Reinventing Space Conference, Belfast, November 2019.

2 SPECIFIC ADVANTAGES OF TMF PANEL TESTS

TMF panel tests offer unique advantages for the validation of CFD, thermal and structural analyses compared to sub- and full scale tests with combustion chambers:

- The heat flux into the wall structure is directly definable through an extensive evaluation of the laser profile, the optical power output of the laser and the absorption at the laser wavelength. Additionally the measurement of the inlet and outlet temperatures of the LN_2 coolant provides a direct opportunity for a caloric evaluation of the total heat flux. In contrast to this the heat flux in combustion chambers is only indirectly determinable by means of caloric evaluation of the coolant.
- The infrared camera provides an accurate 2-dimensional temperature field of the heated wall section. These data can be both a valuable validation of a coupled CFD and thermal analysis and also serve as an input boundary condition in a structural analysis. For combustion chambers it is usually only possible to obtain temperature data from single thermocouples inside the combustion chamber wall but not at its surface. Furthermore thermocouples can only provide single spot measurements.
- The possibility of measuring the 2-dimensional displacement field with its 3 components (u_x, u_y, u_z) with an optical stereo camera system permits the evaluation of

the deformation before, during and after each laser cycle. Particularly the evolution of the deformation during the laser-on time is a unique capability. In combustion chambers the deformation is usually only determinable before or after each hot run.

- Through the usage of nitrogen as coolant, the safety of the overall test installation is strongly increased. The nitrogen is neither flammable nor explosive, whereas hydrogen or also methane in combustion processes always need higher safety regulations. These lower safety regulations also come along with significantly lower costs for maintenance and operation.
- TMF panel tests support the evaluation of only the mechanical and thermal loads, i.e. the thermally induced stress and strain, creep and thermal ageing. In contrast to this, fatigue life tests with combustion cannot be separated from other influences like chemical effects caused by the propellants (blanching, hydrogen embrittlement), abrasive effects caused by the hot gas or pressure and temperature fluctuations caused by combustion instabilities.
- With different designs of TMF panels, the combustion chamber material can be evaluated for different cyclic strain values.

3 THE DOGHOUSE EFFECT IN LIQUID ROCKET ENGINES

The inner copper or copper alloy liner of a regeneratively cooled liquid rocket engine combustion chamber has to endure inelastic strains and creep phenomena caused by high temperature gradients and pressures during each operational cycle. This leads to an accumulation of deformation that eventually induces a progressive thinning of the cooling channel hot gas wall. Furthermore thermal ageing reduces the stress level and the failure strain of the material. The characteristic effect developing from a rectangular shape (see Fig. 1a) of the cooling channel over an almost roof-shaped contour (Fig. 1c) towards the final crack (Fig. 1d) is called "doghouse-effect" [5].

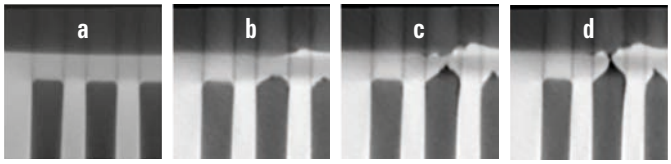

Fig.1 Evolvement of the doghouse-effect in the recently tested third-generation TMF panel of a CuCrZr alloy (CT-Scan).

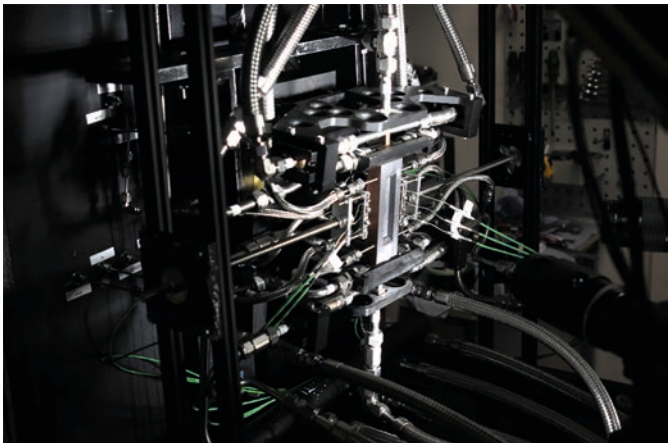

Fig. 2: Third-generation combustion chamber type TMF panel mounted inside the TMF panel test bench.

4 HISTORY OF TMF PANEL TESTS

The first thermomechanical test bench with a TMF panel dedicated to rocket nozzles was set up by Carden [6] in 1966 to study thermal fatigue effects in a nozzle of a nuclear rocket engine. For the fatigue life analysis of the thrust chamber during the development of the Space Shuttle Main Engine (SSME) in the 1970s several sub-scale thrust chambers still were tested to failure by Quentmeyer [9].

In Europe a TMF panel based analysis of the fatigue life of the Vulcain 2 nozzle was first successfully carried out during the Ariane 5 Flight Recovery Programme (FRP) in 2003 and 2004 [2]. The TMF panel test bench at DLR Lampoldshausen was implemented in 2006 and 2007, in the first instance serving as a validation opportunity for numerical simulations of nozzle structures. The focus was then shifted towards the inner liner of combustion chambers and the evaluation of the previously described doghouse-effect. The different properties, shapes and generations of the combustion chamber-like TMF panels (Fig.2) that have been evaluated at DLR Lampoldshausen are shown in Table 1.

TABLE 1 Overview of TMF Panel History at DLR Lampoldshausen

	1st generation	2nd generation	3rd generation
Material	**CuCrZr**	**CuCrZr**	**CuCrZr**
Manufacturing	Cast + annealed + rolled + galvanic deposited nickel layer	Cast/ annealed/ rolled	Cast/annealed/ rolled
Total size	100 mm x 400 mm x 20 mm	33 mm x 200 mm x 18 mm	48 mm x 230 mm x 20 mm
Number of cooling channels	5	7	5 + 2
Wall thickness	1 mm		
Channel width	1 mm	1.3 mm	
Channel height	10 mm	9 mm	
Fillet width	1 mm		
Cyclic strain @ Tmax		≈1 %	≈2 %
Laser loaded surface	planar	Cylindrical, r = 130 mm	
Status	Tested in 2013	Tested in 2018	Tested in 2019

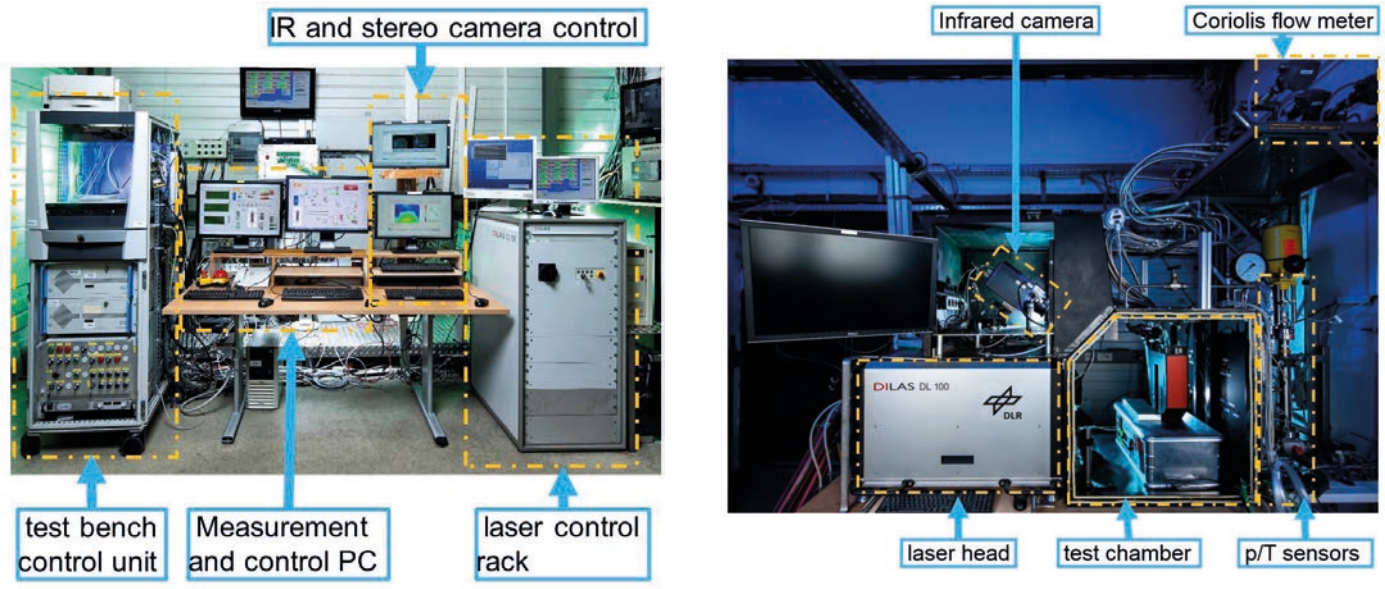

Fig.3 Control room (left) and test cell (right) of the DLR Lampoldshausen TMF panel test bench.

5 COMPONENTS OF THE TMF PANEL TEST BENCH

The TMF panel test bench at DLR Lampoldshausen (Fig. 3) comprises several structurally separated components. These are mainly the control room, the test cell room and fluid supply and dump systems. Particularly the separation of the laser in an enclosed room is a safety requirement.

5.1 High Power Diode-Laser

The exceptionally high heat flux densities through the combustion chamber wall of liquid rocket engines (up to 80 MW/m² in the nozzle throat of the Vulcain main engine [4]) demand special heating devices also for the TMF test bench in order to achieve similar conditions.

In [6], Carden used Quartz lamp radiant heaters providing a heat flux of approximately $\dot{q}$ = 1.1 MW/m² which is still an order of magnitude too low. Apart from high pressure combustion, the only available source for such high heat flux densities is by laser. In combination with a coating featuring a high coefficient of absorptivity one can achieve heat flux densities of up to $\dot{q}$ = 25 MW/m². Table 2 displays the technical parameters of the diode laser of the TMF panel test bench at DLR Lampoldshausen. It was manufactured by DILAS in 2007 [3].

The output power of the laser is controlled via the software of the TMF panel test bench. The function of output control voltage between U = 1.1…6.0 V corresponds to the power density in the focal plane as:

$$\dot{q}_{\mathrm{Laser}}(\mathrm{U}) = -6.54\,\frac{\mathrm{MW}}{\mathrm{m}^2} + 5.80\ \mathrm{U\ MW/(m^2V)}$$

The overall output power is measured with a PRIMES PowerMonitor with an accuracy of ± 3 % and a reproducibility of ± 1 %.

The laser profile itself is characterized in the focal plane with a PRIMES BeamMonitor BM 100 for different control voltages. The accuracy of the BM 100 is ± 5 % for the distribution of the intensity of the laser beam. It can measure the laser beam with a resolution of up to 128 x 256 pixels which represents 0.26 x 0.26 mm/pixel.

TABLE 2 Technical parameters of DILAS diode laser

Parameter	Symbol	
Laser wavelength	λ	940 ±10 nm
Optical power	P	11 kW
Focal plane	A	10 mm x 30 mm
Focal distance	l	399 mm
Homogeneity		< ± 5%
Maximum Power Density	q	28 MW/m²

Fig.4 PRIMES PowerMonitor and BeamMonitor.

Fig.5 FLIR SC7000 Series Infrared Camera.

5.2 Infrared Camera FLIR

During the laser heating phases the 2-dimensional surface temperature is measured in real time by a FLIR SC7000 series infrared camera. The resolution is 640 x 512 pixels. Although frame rates of up to 100 Hz are possible, a frame rate of only 4 Hz is used for the TMF panel tests. The accuracy is ± 1 % or ± 1 K. The infrared camera measures the temperature by using a narrow band filter with a wavelength of λ_{IR} = 3.99 µm. To avoid any influence of reflected laser light, a λ_{hp} = 2.5 µm high pass filter made of Germanium is mounted between the test chamber and the IR camera. By regulating the laser control voltage according to the infrared camera's image the surface temperature can be controlled with a display accuracy of ± 1 K.

5.3 LIMESS Stereo Camera System for Deformation Measurement

To obtain the deformation of the TMF panel surface during a laser hot run as well as the development of the deformation increment between laser cycles a stereo camera system is used. Two 16-megapixel cameras provide high resolution imagery with a frequency of up to 3 Hz. A digital image correlation software determines the 3 displacement components (u_x, u_y, u_z) in a 2-dimensional section. Therefore speckle marks are applied to the surface with an airbrush system before the very first laser-on phase of the TMF panel test.

5.4 The TMF Panel Test Bench Fluid System

For safety reasons and also cost efficiency the TMF panel test bench is operated with supercritical Nitrogen as coolant in contrast to the widely used hydrogen, kerosene or methane coolant in full scale LRE. To achieve the cryogenic test conditions of T = 160 K and p = 50 bar the TMF panel test bench is using both gaseous nitrogen and liquid nitrogen, respectively. The GN_2 is being provided at ambient temperature by the general supply of DLR site Lampoldshausen whereas the LN_2 is stored in a nearby tank and fed into the fluid system with a high pressure piston pump. Both components are mixed in order to achieve the desired test condition and then split into seven feed lines, one for each cooling channel. The mass flow rate of each of these seven feed lines can be individually controlled by the computer via regulating valves. This avoids a non-equal distribution of these seven partial mass flow rates by thermal blockage effects in the center cooling channels of the TMF panel.

The mass flow is measured within each feed line by a separate Coriolis flow meter which allows a mass flow rate control accuracy of ± 0.2 g/s per cooling channel.

5.5 Sensors for Temperature and Pressure Measurement

In order to gain data for the validation of a CFD analysis of the fluid flow inside the TMF panel the temperature and pressure are measured at several positions (see Fig. 6).

The temperature of the supercritical nitrogen is measured at the inlet of cooling channel 4 and at the outlet of each of the 7 cooling channels with type K thermocouples. A single inlet temperature measurement is considered to be sufficient because all cooling channels are fed by the same fluid system. However, the outlet temperature can vary extremely, depending on the different local heat flux values into each of the seven cooling channels of the TMF panel.

Furthermore the surface temperature is measured with thermocouples on 9 dedicated positions around the side and backside of the TMF panel in order to create validation data for the thermal FE analysis of the TMF panel.

The absolute pressure of the coolant is also measured at 8

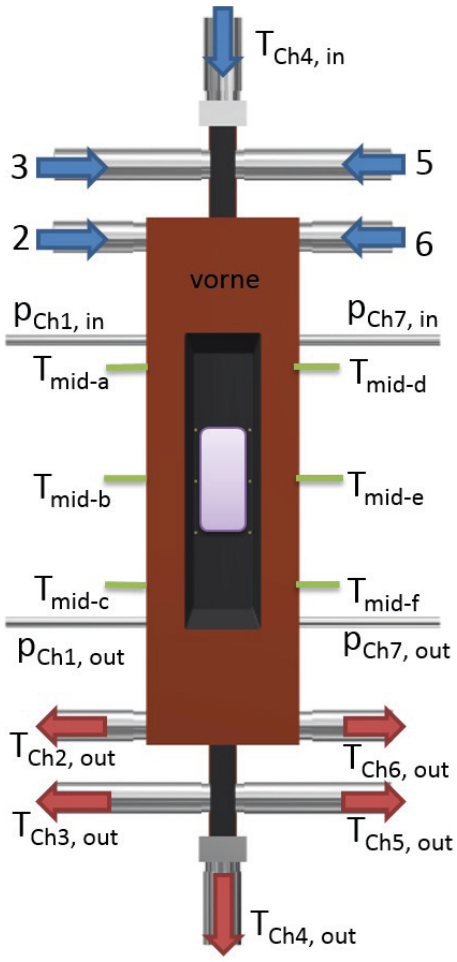

Fig.6 Overview of Sensor Locations, $T_{mid-(g-j)}$ and $T_{Ch(1,7),out}$ are located on the back side of the TMF Panel and not visible in this overview.

positions, one sensor is attached to the inlet of cooling channel 4, and the remaining 7 sensors are measuring the absolute pressure at the outlet of each cooling channel.

Additionally each of the seven cooling channels of the TMF panel is equipped with a differential pressure sensor. The distance of the measurement points is due to limitations according to the construction of the TMF panel between 88.26 mm and 105.26 mm depending on the number of the cooling channel.

6 COMPARISON OF CONDITIONS IN A LOX/LH_2 COMBUSTION CHAMBER AND TMF PANELS

The fatigue life of combustion chambers is dominated by the conditions inside the combustion chamber as well as in the cooling channels. It is therefore necessary to gain validation data for the numerical simulations which are as close to a real combustion chamber as possible but also with justifiable costs. The TMF panel test bench at DLR Lampoldshausen is capable of providing both. A comparison of the conditions for the test bench and a LOX/LH_2 rocket engine throat are listed in Table 3.

7 RESULTS OF THE LATEST 3RD GENERATION TMF PANEL TEST

The latest test at the DLR Lampoldshausen test bench was conducted with a 3rd generation TMF panel made of CuCrZr in the framework of the in house AKIRA project of DLR. The AKIRA project focused on increasing the TRL level of critical technologies for reusable launch vehicles such as insulation, rocket engine components and lightweight structures.

In [7] Thiede developed the theoretical framework for a state of the art FE analysis of both the 2nd generation and the 3rd generation TMF panel. For the 3rd generation TMF panel, the cyclic strain was increased from $\Delta\varepsilon_{2G} = 1$ % to $\Delta\varepsilon_{3G} = 2$ % (see Table 1).

The test conditions for the 3rd generation TMF panel test are shown in Table 3. Each cycle was executed with a laser-on time of 200 s which is approximately the burn time of a liquid rocket booster engine. To decrease the large strain rates at the beginning and end of each cycle, that would be caused by instantly switching the laser on and off, the laser was ramped up and down linearly over 10 s at the start and the end of each laser cycle so that the total duration of a laser loading cycle is 220 s.

The objectives of the test were as follows:

- Validation of the damage parameter based FE analysis of Thiede [7]
- Achieve the doghouse effect as close to real LRE as possible
- Check the behavior regarding design and construction of the 3rd generation TMF panel made from CuCrZr ahead of the follow up tests made of Cu-HCP

In the following sections, some of the results of the TMF panel test are presented.

7.1 Data from the central cooling channel 4 for selected cycles

In [7], Thiede calculated the mass flow rate required per cooling channel to reach $T_{surface} = 1000$ K and a heat flux of $\dot{q} = 20$ MW/m² to $\dot{m} = 9.9$ g/s. As the heat flux was increased to $\dot{q} = 25$ MW/m², a conservative approach to not damage the panel by overheating was chosen and therefore, the mass flow rate in the first laser-on cycle was set to $\dot{m} = 25$ g/s for each of the seven cooling channels of the TMF panel. Therefore the surface temperature could only rise as high as $T_{surface,\ cyl} = 853$ K in the very first laser-on cycle of the TMF panel test. During the next cycles the mass flow rate was constantly decreased so that within cycle 4 the preset surface temperature as well as the heat flux were achieved at the same time.

Due to the (intentionally) increasing damage in the TMF panel material and the deterioration of the thermal conductivity of the CuCrZr caused by this damage, the mass flow rate had to be increased to $\dot{m} = 30$ g/s per cooling channel during the course of the test campaign (see Fig. 9) to prevent the maximum surface temperature rising above $T_{surface} = 1000$ K. Accordingly, the outlet temperature of the coolant decreased with increasing mass flow rate (see Fig. 7). The corresponding development of the coolant pressure is shown in Fig 78.

However, the mass flow rate had to be limited to $\dot{m} = 30$ g/s per cooling channel from cycle 112 on. This eventually led to a local rise of the surface temperature as high as $T_{surface} = 1300$ K (see Fig. 10).

The intended crack ultimately occurred during cycle 215 of the TMF panel test.

TABLE 3 Comparison of Conditions in a LOX/LH2 Combustion Chamber and Supercritical Nitrogen Cooled TMF Panels

Condition	LOX/LH2 engine	TMF test bench
Surface temperature of heat loaded wall	1000 K	1000 K ±1 K
Heat flux through heat loaded wall	80 MW/m²	25 MW/m²
Coolant	LH_2	LN_2
Temperature of coolant	21 K	160 K
Pressure of coolant	160 bar	50 bar
Pressure in combustion chamber/ ambient pressure	100 bar	1 bar
Pressure difference combustion chamber <-> cooling channel	60 bar	49 bar

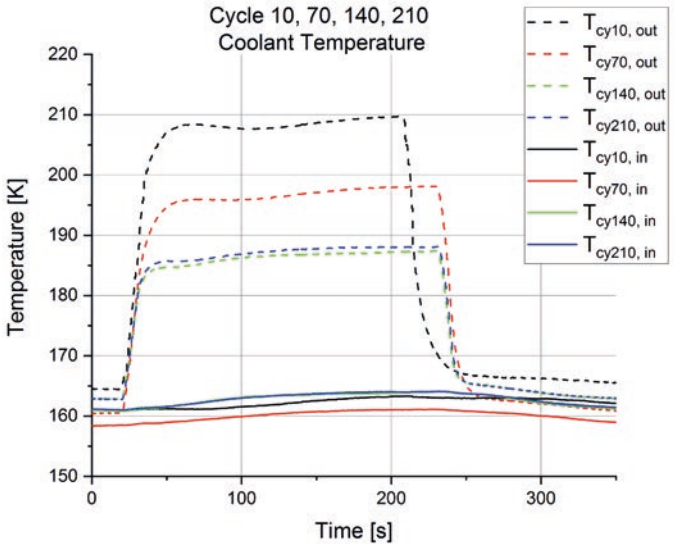

Fig.7 Outlet and Inlet Temperature of Supercritical N_2 Coolant in Cooling Channel 4 for Laser-on Cycles 10, 70, 140 and 210.

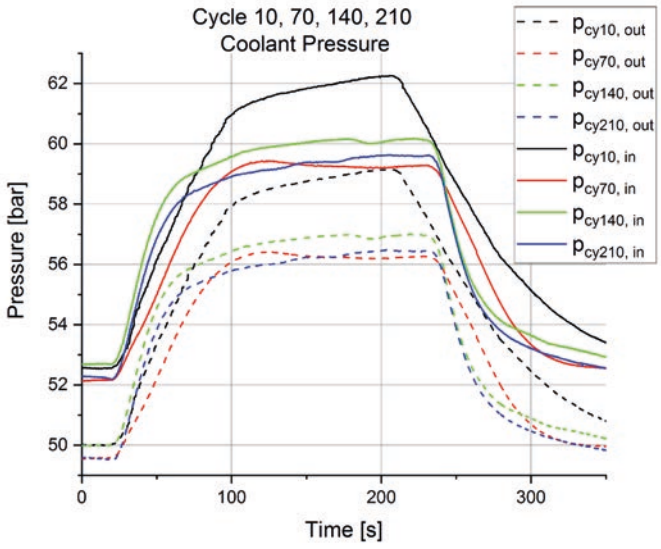

Fig.8 Outlet and Inlet Pressure of Supercritical N_2 Coolant in Cooling Channel 4 for Laser-on Cycles 10, 70, 140 and 210.

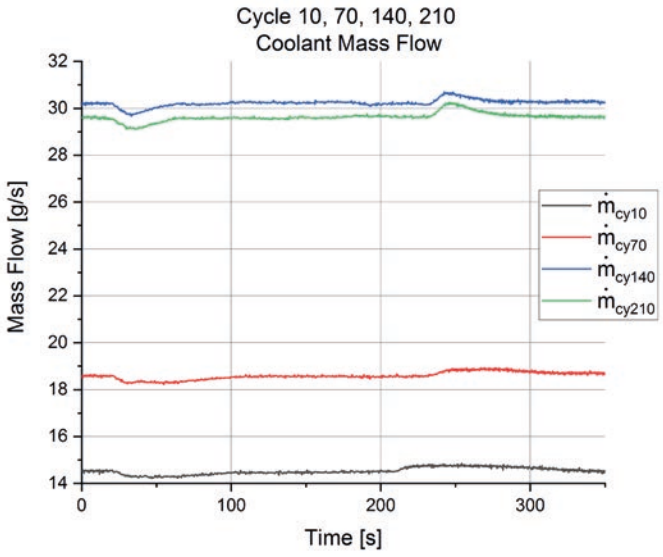

Fig.9 Mass Flow of Supercritical N_2 Coolant in Cooling Channel 4 for Cycles 10, 70, 140 and 210.

Fig.10 **(continued overleaf)**

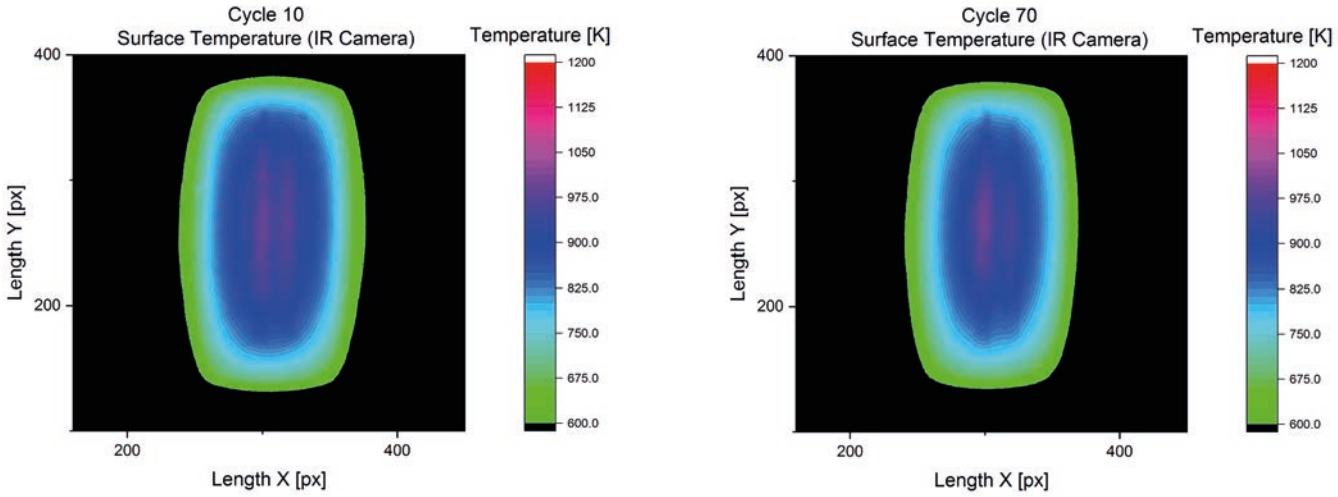

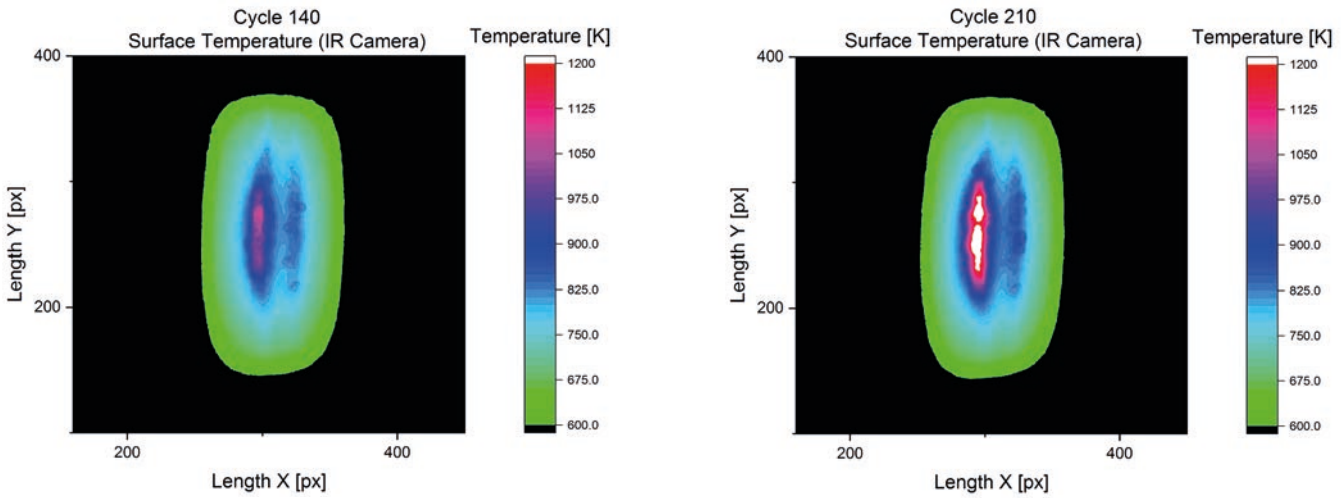

Fig.10 Thermography Images at the End of Cycles 10, 70, 140 and 210 (Scale According to Fig. 15).

7.2 Data for Cooling channel 1 – 7 for Exemplarily Chosen Cycle 75

Figs. 11 to 15 display the measurements of cycle 75 as an example for a typical laser-on cycle.

Particularly Fig. 13 provides valuable data for the validation of a numerical thermal analysis. It displays the previously mentioned temperature measurements on the surface of the TMF panel (see Fig. 6). As sensors $T_{mid\text{-}a}$ and $T_{mid\text{-}d}$ are on the same axial (as referred to a real LRE) position both indicate the same temperature. The same should apply to both sensor couples $T_{mid\text{-}b}$ and $T_{mid\text{-}e}$ as well as $T_{mid\text{-}c}$ and $T_{mid\text{-}f,}$ respectively. However, there are small variations indicating a non-symmetrical heat flux inside the TMF panel. This hypothesis is supported by Fig. 15, as it additionally represents a higher temperature left from the central point in the laser heated area. This effect is increasing during the following laser-on cycles (see Fig. 6).

Another interesting effect is shown in Fig. 14, the mass flow rate in each of the 7 cooling channels decreases by about 0.5 g/s immediately after the laser is switched on. It then slowly increases again to the preset level, before decreasing again but with a much smaller slope. In accordance with this effect, Fig. 11 shows that the outlet temperature of the coolant has a local minimum around 100 s into the cycle. In the IR video footage it can be seen that the surface temperature also rises, when the mass flow rate decreases and vice versa.

7.3 CT-Scan of the crack

In Fig. 1 the results of a CT-scan conducted at the DLR Institute of Structures and Design in Stuttgart are displayed. As already described previously, the development of the damage in the cooling channel wall is observable from subfigures (a) to (d).The doghouse effect is clearly visible. Thus this test objective can be regarded as successful.

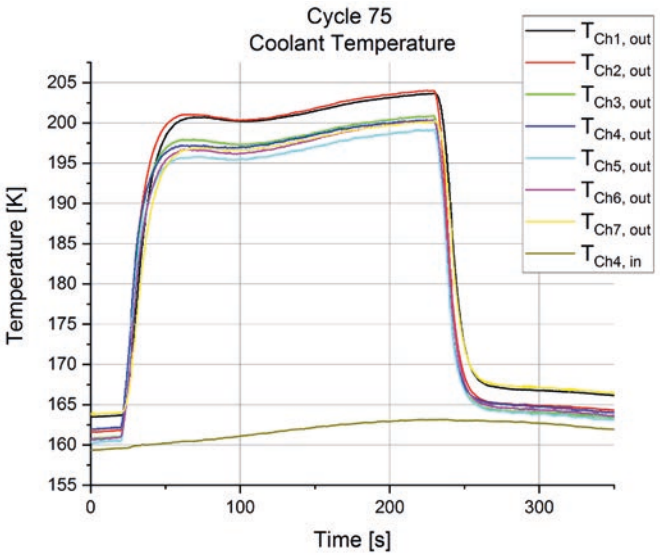

Fig.11 Outlet temperature of cooling channels 1 – 7 and inlet temperature of cooling channel 4 of supercritical N_2 coolant during laser-on cycle 75.

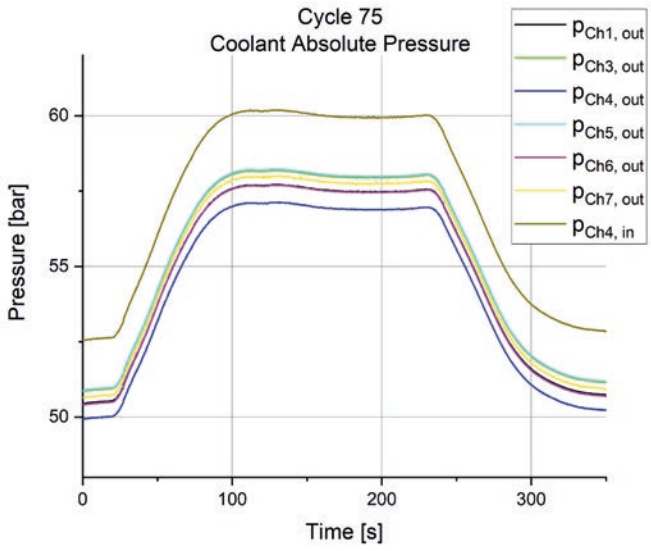

Fig.12 Outlet pressure of cooling channels 1 - 7 and inlet pressure of cooling channel 4 of supercritical N_2 coolant during laser-on cycle 75.

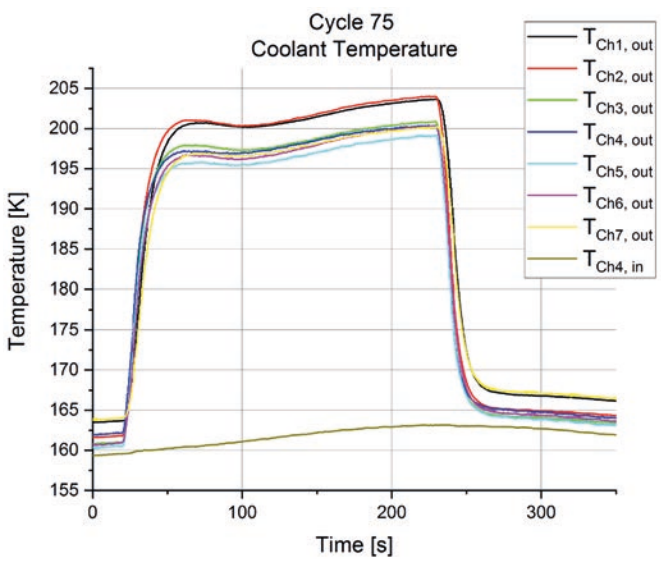

Fig.13 Surface temperatures of the TMF panel during laser-on cycle 75, sensor locations according to Fig. 6.

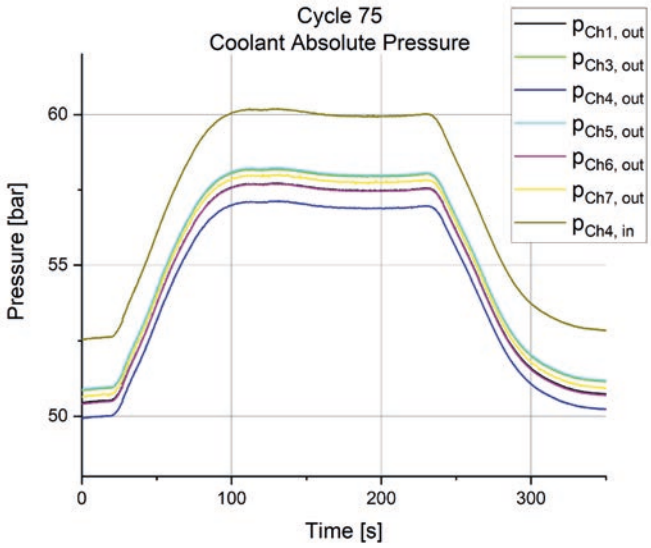

Fig.14 Mass flow rates of supercritical N_2 coolant in cooling channels 1 - 7 during laser-on cycle 75.

Furthermore the crack occurred in cooling channel 3. Thiede also predicted in his simulations that the damage initiation point will be in cooling channel 3. Hence, also the 2nd test objective of validating Thiede's damage parameter based FE analysis is met successfully. Fig. 1 displays cooling channels 3–5.

8 SUMMARY

The present paper explains the unique capabilities of the TMF panel test bench at DLR Lampoldshausen. Additionally the advantages of TMF panel tests compared to subscale or full scale chamber tests based on combustion were discussed. Finally the latest results of the 3rd generation TMF panel were presented. These results are in good conformity with the numerical simulations of Thiede. Therefore the TMF panel test can be seen as an economic and safe approach to gather validation data for the fatigue life of liquid rocket engines as well as for CFD simulations regarding the coolant flow in the regenerative system of real combustion chambers.

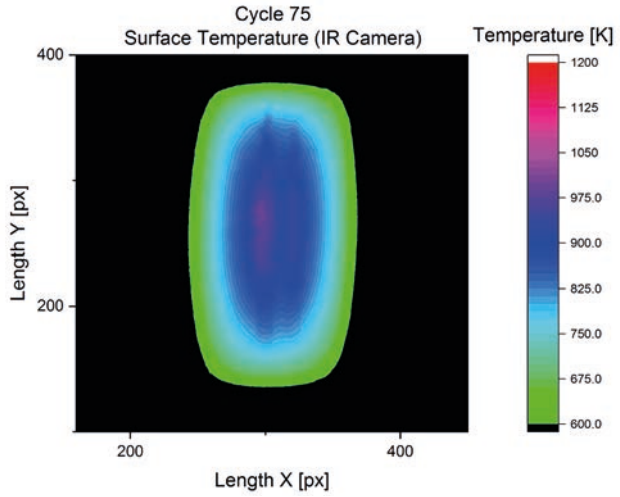

Fig.15 Thermography image of laser heated area of the TMF panel at the end of cycle 75.

Acknowledgements

The authors would like to thank Andreas Gernoth and Ingo Dörr for the construction of the TMF panel test facility and Gordan Thiede and Philipp Kron for the further enhancements realized during the last few years.

REFERENCES

1. A. Gernoth, M. Wurdak, J. Riccius, S. Schlechtriem, D. Wiedmann, W. Schwarz, L. Brummer, "TMF test based validation of numerical methods for the analysis of heat loaded walls," *46th AIAA/ASME/SAE/ASEE Joint Propulsion Conference & Exhibit 2010*, Nashville, TN, USA. 2010.
2. J. Riccius, A. Gernoth, E. Suslova, C. Böhm, E. Zametaev, O. Haidn, L. Brummer, B. Mewes, O. Knab, M. Terhardt, and G. Hagemann, "TMF: Laser Application for a Close-to-Reality Simulation of Thermo-Mechanical Fatigue Processes in Rocket Engines," *2nd European Conference for Aerospace Sciences (EUCASS), Brussels, Belgium, July 2007.*
3. B., Köhler, A., Noeske, T. Kindervater, A. Wessollek, T. Brand and J. Biesenbach,. "11 kW direct diode laser system with homogenized 55 x 20 mm² Top-Hat intensity distribution," *Photonics West*, San Jose, CA, USA. 2007.
4. D. Suslov, A. Woschnak, D. Greuel, and M. Oschwald, "Measurement Techniques for Investigation of Heat Transfer Processes at European Research and Technology Test Facility P8," *European Conference for Aerospace Sciences (EUCASS), Moscow, Russia. 2005.*
5. V. K. Arya, and S. M. Arnold, "Viscoplastic Analysis of an Experimental Cylindrical Thrust Chamber Liner", AIAA Journal, Vol. 30, No. 3, 1992.
6. A. E. Carden, D. G. Harman, E. A. Franco-Ferreira, "Thermal Fatigue Analysis of a Cryogenically Cooled Rocket Nozzle," Technical report. Oak Ridge National Laboratory, TN, USA. 1966.
7. R. G. Thiede, "Validation of Damage Parameter Based Finite

Element Fatigue Life Analysis Results to Combustion Chamber Type Thermomechanical Fatigue Panel Tests," Dissertation, RWTH Aachen University, Aachen, Germany. 2019.

8. W. Schwarz, S. Schwub, K. Quering, D. Wiedmann, H. W. Höppel, M. Göken, "Life prediction of thermally highly loaded components: modelling the damage process of a rocket combustion chamber hot wall," *Council of European Aerospace Societies (CEAS) Space Journal,* Vol. 1, No. 1-4, 2011. 2011.

9. R. J. Quentmeyer, "Experimental fatigue life investigation of cylindrical thrust chambers," Technical. report. NASA-TM-X-13665, NASA Lewis Research Center, 1977.

Received 19 March 2020 **Approved** 2 April 2020